


**COVER PAGE**

***Document downloaded by @DAEL***

***Fri Nov 27 09:01:21 2026***

***For personal use***

When automatic English translation is provided, only the original document is authentic.

The EAA cannot be held responsible of any translation error

Bibliographical reference

*Determination of Vibration Reduction Indices Using Wave Theory for Junctions in Heavyweight Buildings*, C. Hopkins, Acta Acustica **vol. 100** (Number 6), 2014, pp. 1056-1066

DOI

https://doi.org/10.3813/AAA.918785

**Acta Acustica united with Acustica**
**Vol. 100 (2014) 1056 – 1066**

DOI 10.3813/AAA.918785

# Determination of Vibration Reduction Indices Using Wave Theory for Junctions in Heavyweight Buildings

C. Hopkins
Acoustics Research Unit, School of Architecture, University of Liverpool, Liverpool, L69 7ZN, UK.
carl.hopkins@liverpool.ac.uk

**Summary**
Airborne and impact sound insulation in buildings can be predicted according to the International Standard, ISO 15712 and the identical European Standard, EN 12354. Calculation of the flanking transmission requires knowledge of the vibration reduction index for which these standards contain empirical data. This paper investigates the vibration reduction index for the specific case of heavyweight buildings built from solid masonry/concrete walls and floors by using wave theory to calculate data for L-, T- and X-junctions. Calculations are carried out assuming only bending wave transmission at the junction as well as bending and in-plane wave transmission at the junction. The results show that the frequency-invariant empirical data in the standards is likely to give rise to errors in the mid- and high-frequency ranges due to the importance of in-plane wave generation at the junction. Regression analysis is used to identify new relationships that are specific to junctions of solid heavyweight walls and floors. For future work these give the potential to re-assess the existence of any bias error using the model in the standards and allow greater insight into the uncertainty associated with the model.

**PACS no. 43.40.At, 43.40.Dx, 43.55.Rg, 43.55.Ti**

## 1. Introduction

For the estimation of airborne and impact sound insulation in buildings a prediction model is described in the International Standard, ISO 15712 Parts 1 and 2 [1] and the identical European Standard, EN 12354 Parts 1 and 2 [2]. Parts 1 and 2 concern the prediction of airborne and impact sound insulation respectively. For brevity, reference will only be made to EN 12354 in the rest of this paper. This model predicts the combination of direct and flanking transmission in the field situation using path analysis based on Statistical Energy Analysis (SEA). This approach follows the work by Gerretsen [3] and can be described as an SEA-based approach using first-order flanking paths, i.e. involving only flanking paths which involve vibration transmission across one junction of walls and/or floors. In the development of these Standards a new parameter was introduced by Gerretsen [4] to facilitate the calculation of flanking transmission. This was the vibration reduction index, $K_{ij}$, which describes the transmission of bending wave vibration across a junction of walls/floors. It is defined as [1, 2]

$$K_{ij} = \overline{D_{\mathrm{v},ij}} + 10\log\left(\frac{L_{ij}}{\sqrt{a_i a_j}}\right), \tag{1}$$

Received 07 July 2014,
accepted 21 August 2014.

where $L_{ij}$ is the junction length between elements $i$ and $j$, $a$ is the equivalent absorption length and $\overline{D_{\mathrm{v},ij}}$ is the direction-averaged velocity level difference.

The equivalent absorption length is given by

$$a = \frac{2.2\pi^2 S}{c_0 T_\mathrm{s}}\sqrt{\frac{f_\mathrm{ref}}{f}} = \frac{\pi^2 S\eta}{c_0}\sqrt{f_\mathrm{ref} f}, \tag{2}$$

where $S$ is the area, $c_0$ is the speed of sound in air, $T_\mathrm{s}$ is the structural reverberation time, $f_\mathrm{ref}$ is a reference frequency of 1000 Hz, $f$ is the frequency, and $\eta$ is the total loss factor.

The direction-averaged velocity level difference, $\overline{D_{\mathrm{v},ij}}$, is calculated from

$$\overline{D_{\mathrm{v},ij}} = \frac{D_{\mathrm{v},ij} + D_{\mathrm{v},ji}}{2}, \tag{3}$$

where $D_{\mathrm{v},ij}$ is the velocity level difference between source element $i$ and receiver element $j$ (and vice versa for $D_{\mathrm{v},ji}$).

EN 12354-1 has an informative annex, Annex E, which contains empirical $K_{ij}$ data for different types of junctions. These are commonly used to carry out predictions due to the lack of experimental data for specific junctions. The literature contains some comparisons of measurements with predictions using EN 12354 Parts 1 and 2 and the empirical $K_{ij}$ data which show satisfactory agreement for airborne and impact sound insulation (e.g. [3, 4, 5]). However, for heavyweight buildings the prediction model has


© S. Hirzel Verlag · EAA

been shown to incur bias errors of up to +10 dB in the airborne sound insulation when compared with matrix SEA which considers all possible transmission paths [6, 7, 8]. Bias errors have not been evident in some comparisons of measured and predicted single-number quantities for airborne and impact sound insulation (e.g. [2, 7, 8, 9]). However, some comparisons do indicate a bias error which could be attributed to the input data [9].

Craik [6] suggests that one possible reason for not observing a bias error in the original work [3] is because the empirical $K_{ij}$ data in EN 12354-1 is based upon measurements that (unintentionally) included flanking transmission from longer flanking paths. Recent work by Hopkins and Robinson [10] using transient and steady-state forms of SEA provides evidence that $K_{ij}$ measurements on heavyweight junctions in both the laboratory and the field will often incur significant errors due to unwanted flanking transmission. In addition, Hopkins and Robinson show that it is essential to use a short evaluation time for structural reverberation times on heavyweight walls and floors. They concluded that the use of simplified experimental SEA (as incorporated in EN ISO 10848-1 [11] for $K_{ij}$ measurements) with total loss factors determined from structural reverberation times with large evaluation ranges, such as $T_{20}$, can appear to give the right answer for structural coupling parameters such as $K_{ij}$, but for the wrong reasons. This is due to the cancellation of two errors; the error in the estimate of the total loss factor and the error due to unwanted flanking transmission.

In the original work by Gerretsen [3] structural reverberation times were measured to try and normalise the vibration level difference, but as this was unsuccessful these reverberation times were subsequently inferred from measurements of the vibration level differences to all the connected walls/floors. This approach overcame the problem that the equipment needed to measure short reverberation times using reverse-filter analysis was not commonly available in the 1970s. Currently, Annex E in EN 12354-1 contains empirical $K_{ij}$ data and states that "These data are deduced from generalized data on the junction velocity level differences as available from literature. The other terms in equation [see equation (1)] are estimated on the basis that the vibration reduction index should be such that for all structural elements and field situations the estimated junction velocity level difference should on average be correct. This resulted generally in values for $K_{ij}$ which are 5 dB lower than the corresponding direction-averaged junction velocity level difference. If other relevant data are available on the junction velocity level difference, the same approach could be used to deduce values for the vibration reduction index $K_{ij}$ for application of the model". Annex E is purely informative, but many users of the prediction model do not have access to measured $K_{ij}$ data for specific types of junctions. For this reason they are widely used as default values, particularly because some of the accompanying diagrams (e.g. T-junction) indicate that they are applicable to a wide range of inhomogeneous or double leaf constructions.

For current and future revisions of EN 12354-1 one consideration is whether the empirical curves should be reformulated for different types of construction. For example, following the publication of EN 12354-1 many researchers measured $K_{ij}$ with inhomogeneous walls and floors such as those incorporating hollow bricks (e.g. [12]), or walls with resilient interlayers (e.g. [13]) and noted significant differences between the empirical $K_{ij}$ data from EN 12354-1 and their measurements. It might therefore be possible to produce separate $K_{ij}$ curves for solid heavyweight elements, combinations of lightweight facades with heavyweight separating walls, hollow brick walls etc. This would make it much easier to assess the accuracy of EN 12354 Parts 1 and 2 for different types of construction.

The aim of this paper is to assess the empirical $K_{ij}$ data contained in Annex E of EN 12354-1 through comparison with $K_{ij}$ data calculated using wave theory for junctions formed from different combinations of homogeneous, isotropic, masonry/concrete walls or floors. The primary reason for considering such plates is that they form the simplest building element, and for that reason it should facilitate future discussions as to why the bias error in the prediction model is not always apparent. The intention with this numerical approach is to circumvent the measurement problems indicated by Hopkins and Robinson [10] that are likely to have led to errors in historical measurements of $K_{ij}$ that formed the basis for the empirical $K_{ij}$ data in these Standards. This can be used to assess whether the empirical $K_{ij}$ data underestimates or overestimates wave theory for common ratios of mass per unit areas and whether the generation of in-plane waves is likely to cause significant frequency-dependence of $K_{ij}$. For the latter, note that the prediction model primarily considers only bending wave energy that is stored in, and transmitted between plate subsystems. Focussing only on bending wave vibration is often assumed to be adequate for transmission paths that cross a junction, but not for non-adjacent rooms involving paths that cross many plate junctions where in-plane waves are important [14].

## 2. Calculation of $K_{ij}$ from wave theory

### 2.1. Relationship between the transmission coefficient and $K_{ij}$

In order to calculate $K_{ij}$ from wave theory it is necessary to relate it to the angular-average transmission coefficient for bending waves on both the source and receiving plates. The direction-averaged velocity level difference for bending wave vibration on two coupled plates can be written in terms of the coupling loss factor $\eta_{ij}$, total loss factors ($\eta_i$ and $\eta_j$) and modal densities ($n_i$ and $n_j$) as [7]

$$\begin{aligned}\overline{D_{\mathrm{v},ij}} &= \frac{D_{\mathrm{v},ij} + D_{\mathrm{v},ji}}{2} \\ &= 10\log\left(\frac{1}{\eta_{ij}}\right) + 5\log\left(\frac{\eta_i \eta_j n_j}{n_i}\right).\end{aligned} \tag{4}$$

Substituting equation (4) in equation (1) gives the vibration reduction index as

$$K_{ij} = -10\log\left(\eta_{ij}\right) + 5\log\left(\frac{\eta_i\eta_j n_j}{n_i}\right) + 10\log\left(\frac{L_{ij}}{\sqrt{a_i a_j}}\right). \quad (5)$$

For bending waves, the modal density for a homogeneous, isotropic plate (thin plate theory) is given by

$$n = \frac{\pi S f_c}{c_0^2}, \quad (6)$$

where $f_c$ is the critical frequency.

The coupling loss factor for bending wave transmission from plate $i$ to plate $j$ is [7]

$$\eta_{ij} = \frac{\tau_{ij} c_{g,i} L_{ij}}{2\pi^2 f S_i}, \quad (7)$$

where $\tau_{ij}$ is the angular-average transmission coefficient for bending wave transmission from plate $i$ to plate $j$, and $c_{g,i}$ is the group speed for bending waves on plate $i$.

Substitution of equations (2), (6) and (7) into equation (5) gives the vibration reduction index in terms of the angular-average transmission coefficient

$$K_{ij} = -10\log\left(\tau_{ij}\right) + 5\log\left(\frac{f_{c,j}}{f_{ref}}\right). \quad (8)$$

An important implication of using equations (6) and (7) in this derivation is that they correspond to two-dimensional bending wave fields on the plate; hence it is only the angular-average transmission coefficient that can be considered, not the normal incidence transmission coefficient. Note that for the local modes of a rectangular heavyweight wall or floor with simply supported boundaries, waves would not impinge upon the junction line at exactly normal incidence over the building acoustics frequency range [7].

### 2.2. Wave theory used to determine the transmission coefficients

In this paper all heavyweight walls and floors are considered to be solid, isotropic, homogeneous plates. For junctions where only bending wave transmission is considered, calculation of the angular-average transmission coefficient is described by Lyon and DeJong [15] and Craik [16]; this results in coefficients that are frequency-invariant. For junctions where there is both bending and in-plane wave generation, major steps in applying the wave approach were made in the work of Cremer *et al.* [17] and Kihlman [18] with subsequent improvements in computing power providing further advances in application and development of the theory for other types of plate junctions [19, 20, 21, 22, 23]. The approach used for the calculations in this paper follows the derivation and calculation procedure described in [7]. The generation of in-plane waves at the junction means that the resulting transmission coefficients for bending wave transmission tend to vary with frequency. Fortunately it is possible to deal with this frequency dependence because for sound insulation in buildings, many general trends can be described by defining the low-, mid-, and high-frequency ranges using one-third octave band centre frequencies where the low-frequency range is 50 Hz to 200 Hz, the mid-frequency range is 250 Hz to 1 kHz, and the high-frequency range is 1.25 kHz to 5 kHz [7]. However, there are rarely any in-plane modes in the low-frequency range, hence only the mid- and high-frequency ranges are considered for which a single value is calculated from the arithmetic average of the vibration reduction index values in those one-third octave bands.

Note that the approach used in EN 12354-1 effectively treats all junctions as a black box by considering only incident and transmitted bending wave fields. If/when there is in-plane wave generation at the junction then the generated in-plane wave energy is assumed not to play any further role in vibration transmission that contributes to the sound radiated into the receiving room.

Assuming that the generation of in-plane waves at the junction is critical, it would be useful if this could be detected during $K_{ij}$ measurements; particularly as these are usually carried out on junctions with complex connections for which no theoretical model is available. From equations (4) and (5) it is seen that the measurement to determine $K_{ij}$ essentially uses a simplified form of Experimental SEA (ESEA) [7]. Hopkins [24] investigated potential methods associated with ESEA to identify wave conversion at the junction using an example of T-junction of solid masonry walls. Three different methods were assessed but the only method with any potential made use of matrix ESEA (rather than simplified ESEA) to calculate and assess the errors in the predicted internal loss factor, and this did not successfully identify wave conversion for all types of junction. This means that it will rarely be possible to identify in-plane wave generation in $K_{ij}$ measurements.

Experimental work and numerical modelling have shown that SEA models using the angular-average transmission coefficient determined from wave theory tend to give close agreement with a single measurement when the larger of the modal overlap factors for two coupled elements is greater than or equal to unity [25, 26, 27, 28, 29]. Fahy and Mohammed [28] also indicate that when using the angular-average transmission coefficient there is another criterion that there should be at least five modes that fall within the frequency band. However, heavyweight walls and floors often have low modal overlap and low modal density for (a) bending modes in the low-frequency range, and (b) in-plane modes in the mid-frequency range [7]. These criteria have been shown to be overly strict for heavyweight walls and floors which tend to be highly damped when fully connected in real buildings [7, 16, 27, 29] and for this reason, it is deemed appropriate to use wave theory.

Table I. Material properties. $c_L$: Quasi-longitudinal wavespeed (m/s), $\nu$: Poisson ratio (-).

| Element type | Material | Thicknesses (mm) | Density (kg/m$^3$) | $c_L$ | $\nu$ |
|---|---|---|---|---|---|
| Floor or Wall | Concrete | 100, 125, 150, 200, 300 | 2200 | 3800 | 0.2 |
| Wall | Aerated concrete blocks | 100, 150, 200, 250, 300 | 800 | 1900 | 0.2 |
| Wall | Aerated concrete blocks | 100, 150, 200, 250, 300 | 400 | 1900 | 0.2 |
| Wall | Lightweight aggregate blocks | 100, 200, 250, 300 | 1400 | 2200 | 0.2 |
| Wall | Dense aggregate blocks | 100, 200, 300 | 2000 | 3200 | 0.2 |
| Wall | Brick | 100, 230 | 1750 | 2700 | 0.2 |
| Wall | Calcium silicate blocks | 100, 250 | 1800 | 2500 | 0.2 |

## 3. Description of heavyweight walls and floors used for the wave theory calculations

To assess the empirical $K_{ij}$ curves in EN 12354-1 the intention in this paper is to carry out wave theory calculations for junctions formed from many different permutations of heavyweight walls and floors and carry out regression analysis.

Junctions of walls and floors are created using the materials described in Table I assuming solid, homogenous, isotropic plates with different thicknesses. This results in 56 L-junctions, 56 T-junctions and 56 X-junctions. For each of the three types of junction, 30 junctions are based around concrete floors with brick/block walls and 26 are based around brick/block walls. For the T-junctions, the cantilever plate is assumed to be a separating wall/floor and the two other plates represent flanking walls/floors with identical thickness and material properties. For the X-junctions, two of the in-line plates are assumed to be separating walls/floors with identical thickness and material properties, and the other two in-line plates represent flanking walls/floors with identical thickness and material properties.

Regression analysis for the wave theory $K_{ij}$ data for each junction has been carried out using the independent variable, $M$, as defined in EN 12354-1 by

$$M = \log\left(\frac{m'_{\perp i}}{m'_i}\right), \tag{9}$$

where $m'_i$ is the mass per unit area (kg/m$^2$) of the element $i$ in the transmission path from $i$ to $j$ and $m'_{\perp i}$ is the mass per unit area (kg/m$^2$) of the other perpendicular element in the junction.

The term in the brackets in equation (9) will be referred to as the ratio of the mass per unit areas. The range of ratios of mass per unit areas shown in the graphs in Annex E of EN 12354-1 is from 0.1 to 30 from which it can be inferred that this indicates the applicability of the empirical equations. However, the realistic permutations for the heavyweight walls and floors described in Table 1 do not span this range: for L- and T-junctions the range is from 0.33 to 16.5 and for X-junctions the range is from 0.1 to 11.

## 4. Results

Figures 1 to 5 contain the results for the L-, T- and X-junctions.

### 4.1. L-junctions

#### 4.1.1. Bending wave theory

For bending only transmission (see Figure 1a), only 5 of the 56 $K_{ij}$ values calculated from wave theory are lower than the empirical $K_{ij}$ curve from EN 12354-1; these were for mass per unit areas between 1.8 and 5. From wave theory, the predicted transmission loss in decibels is lowest when both plates have the same thickness and the same material properties. This occurs for 6 of the 56 plate junctions and although the angular-average transmission coefficient is identical in each case, $K_{ij}$ has different values due to the inclusion of the critical frequency in equation (8). For these 6 junctions where the ratio of the mass per unit areas is unity, this results in $K_{ij}$ values between $-1.5$ dB and $+2.4$ dB for which the critical frequencies of the plates in these junctions range from 57 to 341 Hz. The lowest $K_{ij}$ value of $-1.5$ dB occurs when both walls/floors have a critical frequency of 57 Hz; this provides the only justification for the empirical curve from EN 12354-1 being as low as $-2$ dB when the mass per unit area is unity. The best fit curve (coefficient of determination, $R^2 = 0.90$; standard error, $s.e. = 1.67$) is given by the cubic expression

$$K_{12} = -11.3M^3 + 25.1M^2 + 0.6M + 1, \quad -0.48 \le M \le 1.22. \tag{10}$$

Equation (10) gives values that are on average $\approx$3 dB higher than the empirical curve from EN 12354-1 where the range is 1.5 dB to 3.7 dB higher. However, the general shape of equation (10) and the empirical curve from EN 12354-1 are similar.

#### 4.1.2. Bending and in-plane wave theory

Wave theory that allows bending and in-plane wave generation at the junction results in higher $K_{ij}$ values than the bending only model (see Figure 1b). For the mid-frequency range, the best fit curve ($R^2 = 0.89$; $s.e. = 1.39$) is given by the cubic expression

$$K_{12} = -8.2M^3 + 18.5M^2 + 1.2M + 3.5, \quad -0.48 \le M \le 1.22. \tag{11}$$

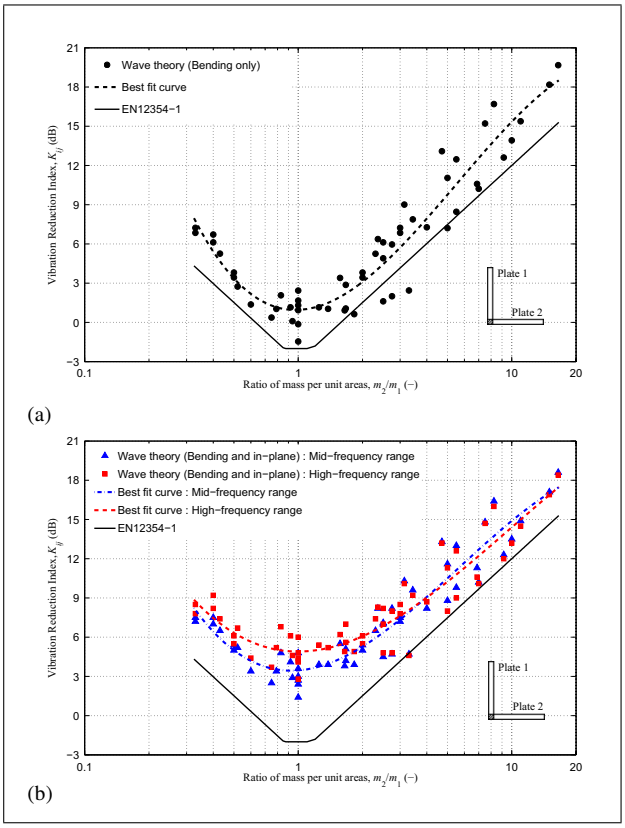


Figure 1. $K_{12}$ for L-junctions. (a) bending wave theory (b) bending and in-plane wave theory.

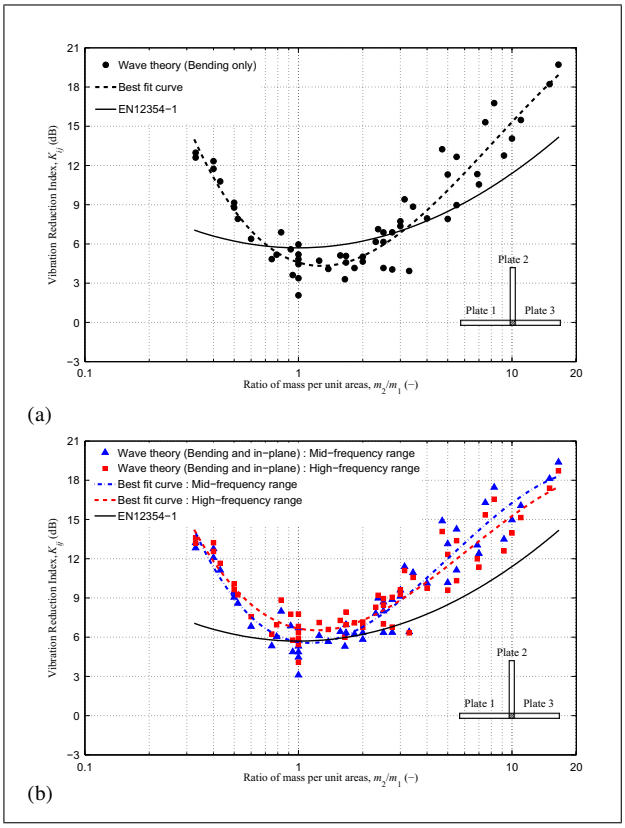


Figure 2. $K_{12}$ for T-junctions (i.e. around the corner). (a) bending wave theory (b) bending and in- plane wave theory. Plates 1 and 3 have identical thickness and material properties.

For the high-frequency range, the best fit curve ($R^2 = 0.84$; $s.e. = 1.44$) is given by the cubic expression

$$K_{12} = -4.8M^3 + 14.3M^2 + 5, \quad -0.48 \leq M \leq 1.22. \tag{12}$$

Compared to the empirical curve from EN 12354-1, equation (11) for the mid-frequency range gives values that are on average 3.2 dB higher (range is 2.2 dB to 5.5 dB higher) and equation (12) for the high-frequency range gives values that are on average 3.4 dB higher (range is 2.2 dB to 7 dB higher). For ratios of the mass per unit area that are less than 3, the $K_{ij}$ values for the mid-frequency range tend to be lower than in the high-frequency range, whereas for ratios greater than 3, the best fit curves for the mid- and high-frequency ranges are similar. Equations (10), (11) and (12) follow a similar cubic form and there is overlap when considering the standard errors, so a single curve representing the average of these three curves might be considered to represent the low-, mid- and high-frequency ranges. However, this would incur significant errors for ratios of the mass per unit areas between 0.5 and 2. One solution would be to use bending only wave theory for the low-frequency range and an average curve based on bending and in-plane wave theory for the mid- and high-frequency ranges.

#### 4.1.3. Discussion

Relatively few examples of measurements on L-junctions of solid heavyweight walls and floors are published in the literature. It can be inferred from L-junction measurements by Craik *et al.* [27] that for transmission from a small wall to a large wall, wave theory would tend to underestimate the actual $K_{ij}$ in the low-frequency range; however, other measurements by Craik [30] indicate that (on average) bending wave theory gives a reasonable estimate. In buildings, the external flanking wall in L- or T-junctions usually contains a window aperture which will slightly increase the $K_{ij}$ value that is calculated from wave theory, and this can be estimated according to [31].

### 4.2. T-junctions

#### 4.2.1. Bending wave theory

Around the corner of the T-junction, Figure 2a shows that 24 of the 56 $K_{ij}$ values predicted using bending wave theory are lower than the empirical $K_{ij}$ curve from EN 12354-1. Around the corner of the T-junctions, the transmission loss in decibels is lowest when both plates have the same thickness and the same material properties. For this reason the lowest $K_{ij}$ value occurs when the ratio of the mass per unit areas is unity although there are a range of values because of different critical frequencies. In addition, it is seen that there is a plateau of low $K_{ij}$ values for ratios between one and three. The best fit curve ($R^2 = 0.89$; $s.e. = 1.43$) is given by the cubic expression

$$K_{12} = -9.1M^3 + 24.8M^2 - 5M + 4.6, \quad -0.48 \leq M \leq 1.22. \tag{13}$$

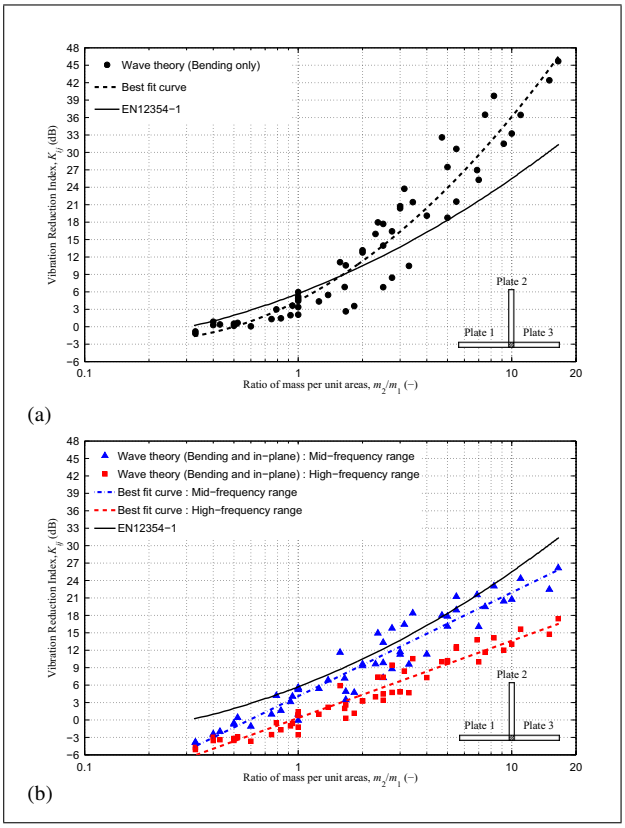


Figure 3. $K_{13}$ for T-junctions (i.e. across the straight section). (a) bending wave theory (b) bending and in-plane wave theory. Plates 1 and 3 have identical thickness and material properties.

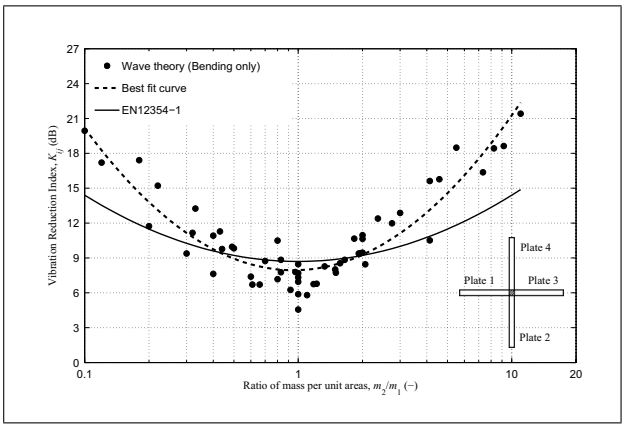


Figure 4. $K_{12}$ for X-junctions (i.e. around the corner). Results are only shown for bending wave theory as they are identical to those for bending and in-plane wave theory. Plates 1 and 3 have identical thickness and material properties. Plates 2 and 4 have identical thickness and material properties.

EN 12354-1 has a quadratic expression with a zero-valued linear coefficient for transmission around the corner of the T-junction. However, it is found that the best fit curve to the wave theory data using a quadratic expression has slightly lower correlation ($R^2 = 0.84$) and therefore it is not considered further in this paper. The curve described by equation (13) is distinctly different to that in EN 12354-1; the latter appears to underestimate $K_{ij}$ values for ratios of the mass per unit area that are less than 0.7 and greater than 3, and overestimate $K_{ij}$ values for ratios between 0.7 and 3. This inconsistency could adversely affect the uncertainty of EN12354-1 calculations for heavyweight buildings because users might expect a consistent bias that would always provide conservative estimates.

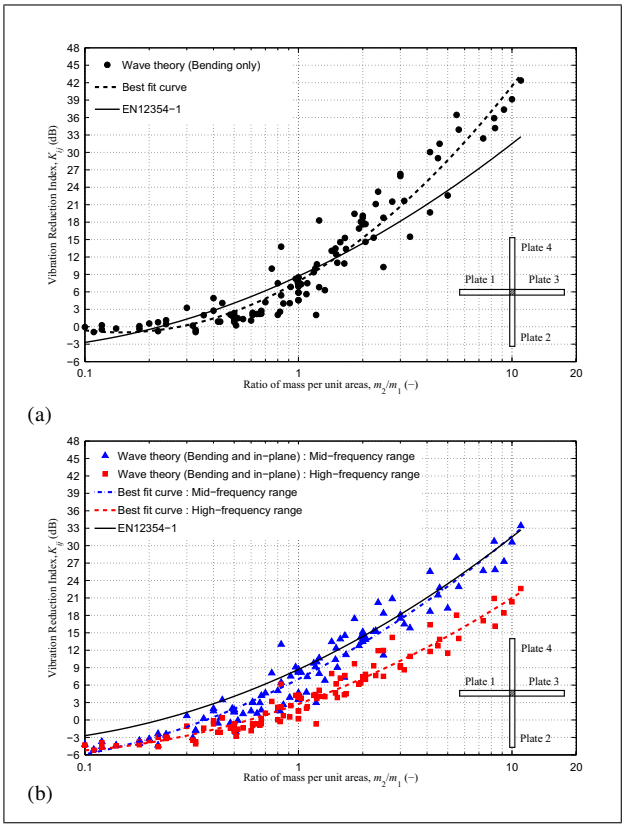


Figure 5. $K_{13}$ for X-junctions (i.e. across the straight section). (a) bending wave theory (b) bending and in-plane wave theory. Plates 1 and 3 have identical thickness and material properties. Plates 2 and 4 have identical thickness and material properties.

Across the straight section of the T-junction, Figure 3a shows that 27 of the 56 $K_{ij}$ values across the straight section of the T-junction are lower than the empirical $K_{ij}$ curve from EN 12354-1; this occurs for ratios between 0.3 and 3.3. The best fit curve ($R^2 = 0.92$; $s.e. = 3.72$) is given by the quadratic expression

$$K_{13} = 12.9M^2 + 18.8M + 4.5, \quad -0.48 \leq M \leq 1.22. \tag{14}$$

For the set of 56 junctions (assuming bending wave theory gives a good estimate of the transmission loss) the tendency is that EN 12354-1 (a) overestimates $K_{ij}$ values both around the corner and across the straight section for ratios of the mass per unit area between 0.7 and 2 and (b) underestimates $K_{ij}$ values both around the corner and across the straight section for ratios greater than 3. For ratios above 3, equations (13) and (14) give significantly higher $K_{ij}$ values than EN 12354-1. The reason for this could be that if field measurements were used to determine the empirical curve in EN 12354-1 these would

be likely to underestimate the actual $K_{ij}$ due to the existence of flanking transmission via other walls and floors [10]; particularly as flanking is likely to become more significant as the ratio of the mass per unit areas increases. However, EN 12354-1 is inconsistent for ratios below 0.7 because it overestimates $K_{ij}$ values around the corner, and underestimates them across the straight section.

#### 4.2.2. Bending and in-plane wave theory

For bending and in-plane wave transmission around the corner of the T-junction (see Figure 2b), the generation of in-plane waves at the junction gives higher $K_{ij}$ values than the bending only model. In the mid-frequency range, the best fit curve ($R^2 = 0.89$; $s.e. = 1.33$) is given by the cubic expression

$$K_{12} = -11.7M^3 + 25M^2 - 2.6M + 5.6, \quad -0.48 \leq M \leq 1.22, \tag{15}$$

and in the high-frequency range, the best fit curve ($R^2 = 0.86$; $s.e. = 1.29$) is given by the cubic expression

$$K_{12} = -8.7M^3 + 20.6M^2 - 3.3M + 6.7, \quad -0.48 \leq M \leq 1.22. \tag{16}$$

As with equation (13) that was derived from bending wave theory, equations (15) and (16) are also distinctly different to the empirical curve in EN 12354-1. However, all three equations follow a similar cubic form and there is overlap when considering the standard errors, so a single curve representing the average of these three curves should provide a reasonable estimate over the low-, mid- and high-frequency ranges.

For transmission across the straight section of the T-junction in the mid-frequency range (see Figure 3b), the best fit curve ($R^2 = 0.92$; $s.e. = 2.34$) is given by the linear expression

$$K_{13} = 17.9M + 4.1, \quad -0.48 \leq M \leq 1.22, \tag{17}$$

and in the high-frequency range, the best fit curve ($R^2 = 0.93$; $s.e. = 1.60$) is given by the linear expression

$$K_{13} = 13.3M + 0.3, \quad -0.48 \leq M \leq 1.22. \tag{18}$$

For transmission across the straight section there is a significant difference between the best fit curve for bending only transmission in equation (14) and bending and in-plane wave transmission in equations (17) and (18) because the latter use a linear rather than a quadratic expression. For the mid- frequency range, equation (17) and the empirical curve from EN 12354-1 are similar for ratios of the mass per unit areas between 1 and 5 (NB For heavyweights walls/floors this range of ratios is common when plate 2 is the separating wall.). However, for the high-frequency range, equation (18) results in significantly lower $K_{ij}$ values than the empirical curve from EN 12354-1.

#### 4.2.3. Discussion

Pedersen [32] tested an isolated T-junction of heavyweight walls and a concrete floor (ratio of mass per unit areas of 3) in the laboratory. For transmission across the straight section there was a decrease in transmission loss with increasing frequency which is indicative of in-plane wave generation at the junction. Around the corner of a T-junction, Pedersen observed that EN 12354-1 appeared to underestimate transmission when compared with measurements and bending and in-plane wave theory.

Hopkins [33] measured isolated T-junctions (masonry walls) in the laboratory but noted that the modal overlap was significantly lower than would exist for fully-connected walls in a real building, and this tended to result in $K_{ij}$ values that were higher than expected and which were therefore unlikely to be situation-invariant. To assess the influence of in-plane wave generation, Hopkins [34] therefore used Finite Element Methods (FEM) to model one of the T-junctions with a ratio of mass per unit areas of 2.2 that was previously measured in the laboratory [33]. Using FEM rather than SEA with wave theory avoided the problematic issue of low-modal overlap. This demonstrated that transmission around the corner was adequately described by bending only FEM models. For transmission across the straight section, bending only and bending and in-plane FEM models were both satisfactory below 800 Hz. However, above 800 Hz, only the bending and in-plane FEM model adequately described transmission across the straight section of the T-junction; hence it was concluded that the generation of in-plane waves at the junction was essential when considering transmission across the straight section. Hopkins [7] subsequently showed that for a similar masonry T-junction that was fully connected to other walls and floors in a flanking laboratory (simulating the field situation with higher modal overlap) that SEA could predict the vibration level difference across the two flanking walls forming the straight section of the T-junction to within 3 dB by considering the bending only model below 800 Hz and the bending and in-plane model above 800 Hz. The implication for the best fit curves determined from wave theory in this paper is that for transmission across the corner and the straight section it should be adequate to use the bending only model for the low- and mid-frequency ranges and the bending and in-plane model for the high-frequency range. Predictions made using EN 12354 Parts 1 and 2 with the empirical $K_{ij}$ curve are likely to incur significant errors in the high-frequency range; this could be investigated in future comparisons of EN 12354 with field measurements on solid, homogeneous walls/floors made from concrete and/or masonry.

Isolated T-junctions of rigidly-connected solid masonry walls have also been tested by Schneider and Fischer [35] and Crispin *et al.* [13] for which some junctions showed evidence of the frequency-dependency that would be expected by the generation of in-plane waves in the mid- and high-frequency ranges. Crispin *et al.* compared measurements with SEA and EN 12354-1 which showed differences between measurement and prediction of up to 8.5 dB

in the frequency-average $K_{ij}$. The implication of isolating the junctions was that the results were prone to the problem of low modal overlap. In addition, it was recently noted by Hopkins and Robinson [10] that significant errors can occur when using isolated junctions to quantify $K_{ij}$ for transmission across the straight section because the low total loss factor of all walls means that the separating wall plays a role in transmitting vibration between the flanking walls. The T-junction of masonry walls measured by Schneider and Fischer had a ratio of mass per unit areas of 3.3 and for transmission around the corner there was reasonable agreement with EN 12354-1 in the low- and mid-frequency ranges. However, in the mid- and high-frequency ranges, EN 12354-1 overestimated $K_{ij}$ across the straight section which is in agreement with the findings indicated by wave theory in this paper.

It should be noted that the empirical curves for T-junctions in EN 12354-1 specifically identify that they not only apply to heavyweight solid walls/floors but also to facade junctions where the flanking walls are thin, lightweight single or double-leaf constructions. Some results are shown in Gerretsen [3] which indicate that some lightweight facades that form T-junctions do not behave as rigid T-junctions. For this reason, the empirical curves in EN 12354-1 apply to a wide range of constructions over a wide range of ratios for the mass per unit areas for which the junction with the flanking walls is not always 'rigid' with generation of in-plane waves in the mid- and high-frequency ranges. Therefore it might be beneficial to create different sets of empirical curves in EN 12354-1. For example, in dwellings where the separating and flanking walls in the T-junction are formed from concrete/masonry and plate 2 is the separating wall, the ratio of the mass per unit areas will typically be between 1 and 5, and because of the differences between empirical curves in EN 12354-1 and the best fit curves from wave theory, improved equations could be developed for this type of heavyweight construction.

For block or brick walls there is evidence that their modular, periodic nature causes a decrease in vibration level with distance [7] at and above 3.15 kHz. This could be the cause of the increase in $K_{ij}$ that is observed with some junctions of solid block walls [13, 33, 35], particularly those walls without mortar in the vertical joints between blocks. It is therefore a confounding factor in identifying the frequency-dependence of $K_{ij}$ in the mid- and high-frequency ranges due to in-plane wave generation. However, the evidence available to-date indicates that the issue of transmission across the straight section of T-junctions formed from bricks and blocks is perhaps not yet completely understood.

### 4.3. X-junctions

#### 4.3.1. Bending wave theory

Around the corner of the X-junction, Figure 4 shows that 26 of the 56 $K_{ij}$ values predicted using bending wave theory are lower than the empirical $K_{ij}$ curve from EN 12354-1. The transmission loss in decibels is lowest when both plates have the same thickness and the same material properties; hence the lowest $K_{ij}$ values occur when the ratio of the mass per unit areas is unity. The best fit curve ($R^2 = 0.85$; $s.e. = 1.60$) is given by the quadratic expression

$$K_{12} = 12.8M^2 + 0.6M + 8, \quad -1 \leq M \leq 1. \tag{19}$$

EN 12354-1 also has a quadratic expression (and as with the T-junction it has a zero-valued linear coefficient) although it tends to underestimate $K_{ij}$ values for ratios of the mass per unit areas that are less than 0.3 and greater than 2.

Across the straight section of the T-junction, Figure 5(a) shows that 60 of the 112 $K_{ij}$ values are lower than the empirical $K_{ij}$ curve from EN 12354-1. The best fit curve ($R^2 = 0.93$; $s.e. = 2.95$) is given by the quadratic expression

$$K_{13} = 12.6M^2 + 21M + 7.8, \quad -1 \leq M \leq 1. \tag{20}$$

Equation (20) shows reasonable agreement with the empirical $K_{ij}$ curve from EN 12354-1 for ratios of the mass per unit areas between 0.1 and 3, but EN 12354-1 tends to underestimate $K_{ij}$ values for ratios above 3.

#### 4.3.2. Bending and in-plane wave theory

For bending and in-plane wave transmission around the corner of the X-junction, allowing in-plane wave generation at the junction does not change the transmission loss from the bending only model when plates 1 and 3 are the same and plates 2 and 4 are the same. The wave theory data is therefore the same as shown on Figure 4. Hence for the mid- and high-frequency ranges, the best fit curves for the bending and in-plane wave model are exactly the same as for the bending only model given by equation (19).

For transmission across the straight section of the X-junction in the mid-frequency range (see Figure 5b), the best fit curve ($R^2 = 0.94$; $s.e. = 2.28$) is given by the quadratic expression

$$K_{13} = 5.8M^2 + 18.8M + 7, \quad -1 \leq M \leq 1, \tag{21}$$

and in the high-frequency range (see Figure 5b), the best fit curve ($R^2 = 0.94$; $s.e. = 1.58$) is given by the quadratic expression

$$K_{13} = 5.1M^2 + 13.1M + 2.8, \quad -1 \leq M \leq 1. \tag{22}$$

For the mid-frequency range, equation (21) is similar to the best fit curve for the bending only model (equation 20) for ratios of the mass per unit areas between 0.3 and 2, and similar to the empirical curve from EN 12354-1 for ratios between 2 and 11. Compared with equation (21), EN 12354-1 tends to overestimate $K_{ij}$ values for ratios below 2 by, on average, 2 dB.

For the high-frequency range, equation (22) is only similar to the best fit curve for the mid-frequency range (equation 21) over a narrow range of ratios of the mass per unit areas between 0.1 and 0.3. Compared with equation (22), EN 12354-1 tends to overestimate $K_{ij}$ values over the entire range of ratios from 0.1 to 11 by, on average, 7 dB (range is 2.5 dB to 10.7 dB).

#### 4.3.3. Discussion

Kihlman compared wave theory calculations for an X-junction with both laboratory and field measurements [18, 36]. For an experimental house that simulated the field situation, Kihlman [36] found that for transmission around the corner of an X-junction from a concrete floor slab to a lightweight concrete wall, the predicted transmission loss was 23 dB but measured values were $\approx$ 6 dB lower than this between 160 Hz and 1.6 kHz. It was postulated that this might have been due to high levels of in-plane wave vibration. However, on the basis of recent calculations [10] this is likely to be attributed to unwanted flanking transmission via other paths. Further evidence to support the possibility of flanking in the aforementioned case comes from other field tests by Kihlman [18] around the corner of an X-junction where transmission was stronger (predicted transmission loss was 11 dB) and the agreement with measurements was closer. Gerretsen [3] later analysed vibration level difference measurements on X-junctions from Kihlman, Gösele and Westphal and drew a single best fit curve through data for both transmission around the corner and across the straight section. However, the wave theory data confirms the approach used in EN 12354-1 which is to have separate curves for these two types of transmission path.

Crispin *et al.* [13] tested an isolated rigid X-junction of solid masonry walls for which the measured data showed good agreement with EN 12354-1 and for which the measured $K_{ij}$ tended to be invariant with frequency between 100 Hz and 2 kHz. However, as discussed in section 4.2.3, there are significant problems in using isolated junctions of heavyweight walls/floors to determine $K_{ij}$.

## 5. Conclusions

Wave theory has been used to determine the vibration reduction index, $K_{ij}$, for different permutations of heavyweight walls and floors that form L-, T- and X-junctions in buildings. These data have been compared with empirical curves in Annex E of ISO 15712-1 and EN 12354-1 which are shown for ratios of the mass per unit areas from 0.1 to 30. However, for concrete walls and floors, and brick/block walls, the upper limit of applicability will typically be a ratio of mass per unit areas of 16.5 as indicated by the realistic permutations of heavyweight walls and floors considered in this paper. Regression analysis using wave theory data allowed comparison with empirical $K_{ij}$ data from Annex E in EN 12354-1. The results show that the frequency-invariant empirical data in the standards is likely to give rise to errors in the mid- and high-frequency ranges due to in-plane wave generation at the junction. It is feasible to generate new empirical curves for junctions that are formed from solid heavyweight walls/floors over (a) the low-frequency range (50 Hz to 200 Hz) using bending wave theory and (b) the mid-frequency range (250 Hz to 1 kHz) and high-frequency range (1.25 kHz to 5 kHz) using bending and in-plane wave theory.

For L-junctions the cubic formulae derived from regression analysis confirm that the general trend of the empirical $K_{ij}$ curve in EN 12354-1 is appropriate. However, EN 12354-1 gives significantly lower values of $K_{ij}$ than wave theory; hence there is potential to use bending only wave theory for the low- frequency range and an average curve based on bending and in-plane wave theory for the mid- and high-frequency ranges. In general, defining $K_{ij}$ curves for L-junctions is simpler than for T- and X- junctions because the former retains the same variation with the ratio of the mass per unit areas regardless of whether in-plane wave generation at the junction is or is not considered. However, L-junctions primarily occur in heavyweight buildings with cavity wall constructions for which the approach using first-order paths in EN 12354 has been shown to be insufficient [8].

In buildings with solid separating walls/floors, T- and X-junctions play an important role in sound transmission between adjacent rooms. For T- and X-junctions the empirical $K_{ij}$ curves in EN 12354-1 show notably different trends for transmission around the corner and across the straight section when compared to bending only and bending and in-plane wave theory. For T-junctions this may occur because the empirical $K_{ij}$ curves in EN 12354-1 apply to T-junctions with lightweight façade walls as well as heavyweight walls/floors. Hence a new set of empirical $K_{ij}$ curves could be considered for T- and X-junctions formed entirely from heavyweight walls/floors. For transmission around the corner of T-junctions, a single curve representing the average of bending only and bending and in-plane wave theory should provide a reasonable estimate over the low-, mid- and high-frequency ranges. For transmission around the corner of X-junctions, a single curve representing bending only wave theory could provide a reasonable estimate over the low-, mid- and high-frequency ranges. For transmission across the straight section of T- and X-junctions, bending only wave theory could be used to define a curve for the low-frequency range and two separate curves based on bending and in-plane wave theory could be used for the mid- and high-frequency ranges.

For heavyweight walls and floors, this paper indicates the extent and potential importance of frequency-dependence for $K_{ij}$. Taking into account the problems that can occur when determining $K_{ij}$ from laboratory or field measurements [10] this suggests that future work should consider the following three issues. Firstly, the potential for including wave theory data for junctions formed entirely from heavyweight walls/floors in EN 12354-1. This would offer the possibility to further assess the extent and existence of a bias error in EN 12354-1 for buildings that are formed from rigidly connected solid masonry/concrete

walls and floors as noted by Craik [6]. Based on SEA models, Craik showed that if the airborne sound insulation for the direct path is $X$ dB, and for all transmission paths it is $Y$ dB, then the sound insulation predicted by EN 12354-1 using just the direct path and the flanking paths involving one junction is approximately $(X + Y)/2$ dB in any frequency band over the building acoustics frequency range. So if $X-Y$ is 10 dB, EN 12354-1 will overestimate the airborne sound insulation by 5 dB. Secondly, whether more guidance can be given on the use of a single-number quantity for $K_{ij}$ as described in Annex A of EN ISO 10848-1 when there is evidence of frequency-dependence. Thirdly, to assess the uncertainty relating to estimates of sound insulation for heavyweight buildings. The results in this paper indicate the uncertainty in $K_{ij}$, and this could therefore be used to form part of uncertainty assessments of EN 12354 Parts 1 and 2 (e.g. see [37]).

## References

[1] ISO 15712:2005: Building acoustics - Estimation of acoustic performance of buildings from the performance of elements. Part 1: Airborne sound insulation between rooms. Part 2: Impact sound insulation between rooms. International Organisation for Standardisation, 2005.

[2] EN 12354:2000: Building acoustics - Estimation of acoustic performance of buildings from the performance of elements. Part 1: Airborne sound insulation between rooms. Part 2: Impact sound insulation between rooms. European Committee for Standardisation, 2000.

[3] E. Gerretsen: Calculation of the sound transmission between dwellings by partitions and flanking structures. Appl. Acoust. **12** (1979) 413–433.

[4] E. Gerretsen: European developments in prediction models for building acoustics. Acta Acustica **2** (1994) 205–214.

[5] D. B. Pedersen: Evaluation of EN12354 part 1 and 2 for Nordic dwelling houses. Building Acoustics **6** (1999) 259–268.

[6] R. J. M. Craik: The contribution of long flanking paths to sound transmission in buildings. Appl. Acoust. **62** (2001) 29–46.

[7] C. Hopkins: Sound insulation. First ed. Butterworth-Heinemann, 2007.

[8] L. Galbrun: The prediction of airborne sound transmission between two rooms using first-order flanking paths. Appl. Acoust. **69** (2008) 1332–1342.

[9] H. Metzen: Accuracy of CEN-prediction models applied to German building situations. Building Acoustics **6** (1999) 325–340.

[10] C. Hopkins, M. Robinson: On the evaluation of decay curves to determine structural reverberation times for building elements. Acta Acustica united with Acustica **99** (2013) 226–244.

[11] EN ISO 10848-1:2006: Acoustics - Laboratory measurement of the flanking transmission of airborne and impact sound between adjoining rooms. Part 1: Frame document. International Organization for Standardization, 2006.

[12] A. Cortes, A. Esteban: Hollow ceramic brick walls in Southern Europe dwellings: Limitations and future perspectives of use. Proceedings of Euronoise, Naples, 2003.

[13] C. Crispin, B. Ingelaere, M. Van Damme, D. Wuyts: The vibration reduction index $K_{ij}$: Laboratory measurements for rigid junctions and for junctions with flexible interlayers. Building Acoustics **13** (2006) 99–112.

[14] R. J. M. Craik, A. Thancanamootoo: The importance of in-plane waves in sound transmission through buildings. Appl. Acoust. **37** (1992) 85–109.

[15] R. H. Lyon, R. G. DeJong: Theory and application of statistical energy analysis. Second ed. Butterworth-Heinemann, Boston, 1995.

[16] R. J. M. Craik: Sound transmission through buildings using statistical energy analysis. First ed. Gower, Cambridge, 1996.

[17] L. Cremer, M. Heckl, E. E. Ungar: Structure-borne sound. Springer-Verlag, 1973.

[18] T. Kihlman: Transmission of structure-borne sound in buildings. Report 9/67. National Swedish Institute for Building Research, 1967.

[19] B. M. Gibbs, C. L. S. Gilford: The use of power flow methods for the assessment of sound transmission in building structures. J. Sound Vib. **49** (1976) 267–286.

[20] P. G. Craven, B. M. Gibbs: Sound transmission and mode coupling at junctions of thin plates. Part I: Representation of the problem. J. Sound Vib. **77** (1981) 417–427.

[21] W. Wöhle, T. Beckmann, H. Schreckenbach: Coupling loss factors for statistical energy analysis of sound transmission at rectangular structural slab joints. Parts I and II. J. Sound Vib. **77** (1981) 323–344.

[22] R. S. Langley, K. H. Heron: Elastic wave transmission through plate/beam junctions. J. Sound Vib. **143** (1990) 241–253.

[23] P. Mees, G. Vermeir: Structure-borne sound transmission at elastically connected plates. J. Sound Vib. **166** (1993) 55–76.

[24] C. Hopkins: Experimental statistical energy analysis of coupled plates with wave conversion at the junction. J. Sound Vib. **322** (2009) 155–166.

[25] H. G. Davies, M. A. Wahab: Ensemble averages of power flow in randomly excited coupled beams. J. Sound Vib. **77** (1981) 311–321.

[26] B. L. Clarkson, M. F. Ranky: On the measurement of the coupling loss factor of structural connections. J. Sound Vib. **94** (1984) 249–261.

[27] R. J. M. Craik, J. A. Steel, D. I. Evans: Statistical energy analysis of structure-borne sound transmission at low frequencies. J. Sound Vib. **144** (1991) 95–107.

[28] F. J. Fahy, A. D. Mohammed: A study of uncertainty in applications of SEA to coupled beam and plate systems. Part 1: Computational experiments. J. Sound Vib. **158** (1992) 45–67.

[29] C. Hopkins: Statistical energy analysis of coupled plate systems with low modal density and low modal overlap. J. Sound Vib. **251** (2002) 193–214.

[30] R. J. M. Craik: The prediction of sound transmission through buildings using Statistical Energy Analysis. J. Sound Vib. **82** (1982) 505–516.

[31] C. Hopkins: Vibration transmission between coupled plates using finite element methods and statistical energy analysis. Part 2: The effect of window apertures in masonry flanking walls. Appl. Acoust. **64** (2003) 975–997.

[32] D. B. Pedersen: Estimation of vibration attenuation through junctions of building structures. Appl. Acoust. **46** (1995) 285–305.

[33] C. Hopkins: Measurement of the vibration reduction index, $K_{ij}$, on free-standing masonry wall constructions. Building Acoustics **6** (1999) 235–257.

[34] C. Hopkins: Vibration transmission between coupled plates using finite element methods and statistical energy analysis. Part 1: Comparison of measured and predicted data for masonry walls with and without apertures. Appl. Acoust. **64** (2003) 955–973.

[35] M. Schneider, H.-M. Fischer: Measurement of the vibration reduction index $K_{ij}$ on masonry walls in the laboratory. Proceedings of ICA, Rome, 2001.

[36] T. Kihlman: Sound transmission in building structures of concrete. J. Sound Vib. **11** (1970) 435–445.

[37] J. Mahn, J. Pearse: On the probability density functions of the terms described by the EN12354 prediction method. Building Acoustics **15** (2008) 263–287.